

Confinement-deconfinement transition in two coupled chains with umklapp scattering

M. Tsuchiizu and Y. Suzumura

Department of Physics, Nagoya University, Nagoya 464-8602, Japan

(Received 4 November 1998)

A role of umklapp scattering has been examined for two-coupled chains with both forward and backward scattering by applying the renormalization group method to the bosonized Hamiltonian. It has been found that a state with relevant interchain hopping changes into a state with irrelevant (confined) one when the magnitude of umklapp scattering becomes larger than that of interchain hopping. The critical value of umklapp scattering for such a confinement-deconfinement transition is calculated as the function of interchain hopping and intrachain interactions. A crossover from one-dimensional regime into that of coupled chains is also shown with decreasing temperature. [S0163-1829(99)11019-1]

I. INTRODUCTION

Quasi-one-dimensional organic conductors, $(\text{TMTSF})_2\text{X}$ and $(\text{TMTTF})_2\text{X}$ salts, exhibit instabilities toward spin Peierls state, spin density wave (SDW) state and superconducting (SC) state, where the phase diagram has been displayed on the plane of effective pressures and temperature.^{1,2} The interplay of low dimensionality and repulsive interaction is important for the SDW state which indicates one-dimensional fluctuations.^{3,4} There are also some evidences for dimensional crossover.⁵

Crystal structure shows quarter filling for conduction electrons but the existence of dimerization leads to a half-filled band.⁶ A crossover from a half-filled band to a quarter-filled one has been found by decreasing dimerization under effective pressure, i.e., the variation of anions X. Electronic properties, which suggest a role of the dimerization, have been reported recently at temperatures just above the SDW state.^{7,8} Optical experiments on a series of the above materials, which have different values of interchain electron-transfer energy, show a correlation gap due to umklapp scattering and a crossover from metallic state to insulating state with increasing the anisotropy. An insulator-to-metal transition followed by the deconfinement of interchain hopping has been observed when the interchain transfer energy exceeds a critical value with a magnitude of the order of the gap.

Theoretical studies of these conductors have been explored by use of quasi-one-dimensional model consisting of an array of chains coupled by interchain hopping. For repulsive intrachain interaction and incommensurate band, the transverse hopping is always relevant for the weak interaction,⁹ but there is a reduction of transverse hopping by one-dimensional fluctuation.¹⁰ Two-coupled chains is a basic model for a quasi-one-dimensional system since both one-dimensional fluctuation and transverse hopping can be studied on the same footing. In a Tomonaga-Luttinger model with only forward scattering, the dominant state remains the same as that of a one-dimensional system, but the degeneracy of in-phase and out-of-phase pairings is removed.¹¹⁻¹⁴ When backward scattering is added, the phase diagram becomes quite different from that of a single chain. In a Hub-

bard model with repulsive interaction and without umklapp scattering, the ground state of two-coupled chains is the *d*-wave-like SC state,^{12,15-17} although that of a single chain is the SDW state.¹⁸ The effect of interchain hopping is much stronger compared with the intrachain interaction since the transverse hopping is relevant except for extremely large intrachain interaction.¹² However, intrachain interaction becomes important as well as the interchain hopping for the case of the spin anisotropic backward scattering where a spin gap induced in a single chain leads to a competition between the SDW state and the SC state.¹⁹

Recently, confinement, which denotes incoherence of single-particle hopping between Luttinger liquids has been maintained,^{20,21} where there is no coherence of hopping and then no split Fermi surface below a critical value of single-particle hopping. The confinement has been argued for the metallic state of organic conductor $(\text{TMTSF})_2\text{X}$ under a magnetic field, which is close to coherence-incoherence transition.²² The role of umklapp scattering, which leads to the relevance and the irrelevance of the correlation gap, has been examined for organic conductors.²³ In terms of a Mott gap, the irrelevance of single-particle hopping has been discussed in a quasi-one-dimensional system.^{24,25} A confinement has been demonstrated in two-coupled chains with half-filled band²⁶ in order to understand a crossover from the metallic state to the insulating state, which has been found at temperatures just above the SDW state of organic conductors.⁸ The weakly coupled half-filled chains with infinite numbers have been also studied by a perturbative renormalization group approach.^{23,27}

In the present paper, such a deconfinement-confinement transition due to umklapp scattering is studied in detail for two-coupled chains with half-filled band by developing the previous paper.²⁶ In Sec. II, formulation is given in terms of bosonized-phase Hamiltonian. Renormalization group equations are derived for coupling constants and response functions. In Sec. III, the critical value for confinement is calculated. A crossover at finite temperatures is also shown. In Sec. IV, we discuss the validity of our present calculation and examine an effect of forward scattering within the same branch.

II. FORMULATION

We consider two-coupled chains given by

$$\begin{aligned}
\mathcal{H} = & \sum_{k,p,\sigma,i} \epsilon_{k,p} a_{k,p,\sigma,i}^\dagger a_{k,p,\sigma,i} - t \sum_{k,p,\sigma} [a_{k,p,\sigma,1}^\dagger a_{k,p,\sigma,2} + \text{H.c.}] \\
& + \frac{g_1}{2L} \sum_{p,\sigma,\sigma',i} \sum_{k_1,k_2,q} a_{k_1,p,\sigma,i}^\dagger a_{k_2,-p,\sigma',i}^\dagger a_{k_2+2pk_F+q,p,\sigma',i} a_{k_1-2pk_F-q,-p,\sigma,i} \\
& + \frac{g_2}{2L} \sum_{p,\sigma,\sigma',i} \sum_{k_1,k_2,q} a_{k_1,p,\sigma,i}^\dagger a_{k_2,-p,\sigma',i}^\dagger a_{k_2+q,-p,\sigma',i} a_{k_1-q,p,\sigma,i} \\
& + \frac{g_3}{2L} \sum_{p,\sigma,i} \sum_{k_1,k_2,q} a_{k_1,p,\sigma,i}^\dagger a_{k_2,p,-\sigma,i}^\dagger a_{k_2-2pk_F+q,-p,-\sigma,i} a_{k_1-2pk_F-q,-p,\sigma,i}, \tag{2.1}
\end{aligned}$$

where t is the interchain hopping energy. The quantity $a_{k,p,\sigma,i}^\dagger$ denotes a creation operator for the electron with momentum k , spin σ ($=\uparrow, \downarrow$ or $+, -$), and chain index i ($=1,2$). The symbol $p=+$ ($-$) represents the right-going (left-going) state. In Eq. (2.1), $\epsilon_{k,p} [=v_F(pk - k_F)]$ is the linearized kinetic energy with Fermi velocity v_F and Fermi momentum k_F . Quantities g_2 , g_1 , and g_3 are coupling constants of intrachain interactions for forward scattering, backward scattering, and umklapp scattering, respectively.

The diagonalization of the first and second terms in Eq. (2.1) is performed by making use of a unitary transformation $c_{k,p,\sigma,\mu} = (-\mu a_{k,p,\sigma,1} + a_{k,p,\sigma,2})/\sqrt{2}$ with $\mu = \pm$. After the bosonization of electrons around the new Fermi point $k_{F\mu} \equiv k_F - \mu t/v_F$ we define the phase variables $\theta_{\rho+}$ and $\theta_{\sigma+}$ (θ_{C+} and θ_{S+}), which express fluctuations of the total (transverse) charge density and spin density.¹⁴ They are given by

$$\theta_{\rho\pm}(x) = \frac{1}{\sqrt{2}} \sum_{q \neq 0} \frac{\pi i}{qL} e^{-\alpha|q|/2 - iqx} \sum_{k,\sigma,\mu} (c_{k+q,+,\sigma,\mu}^\dagger c_{k,+,\sigma,\mu} \pm c_{k+q,-,\sigma,\mu}^\dagger c_{k,-,\sigma,\mu}), \tag{2.2}$$

$$\theta_{\sigma\pm}(x) = \frac{1}{\sqrt{2}} \sum_{q \neq 0} \frac{\pi i}{qL} e^{-\alpha|q|/2 - iqx} \sum_{k,\sigma,\mu} \sigma (c_{k+q,+,\sigma,\mu}^\dagger c_{k,+,\sigma,\mu} \pm c_{k+q,-,\sigma,\mu}^\dagger c_{k,-,\sigma,\mu}), \tag{2.3}$$

$$\theta_{C\pm}(x) = \frac{1}{\sqrt{2}} \sum_{q \neq 0} \frac{\pi i}{qL} e^{-\alpha|q|/2 - iqx} \sum_{k,\sigma,\mu} \mu (c_{k+q,+,\sigma,\mu}^\dagger c_{k,+,\sigma,\mu} \pm c_{k+q,-,\sigma,\mu}^\dagger c_{k,-,\sigma,\mu}), \tag{2.4}$$

$$\theta_{S\pm}(x) = \frac{1}{\sqrt{2}} \sum_{q \neq 0} \frac{\pi i}{qL} e^{-\alpha|q|/2 - iqx} \sum_{k,\sigma,\mu} \sigma \mu (c_{k+q,+,\sigma,\mu}^\dagger c_{k,+,\sigma,\mu} \pm c_{k+q,-,\sigma,\mu}^\dagger c_{k,-,\sigma,\mu}). \tag{2.5}$$

There is a commutation relation that $[\theta_{\nu+}(x), \theta_{\nu'-}(x')] = i\pi \delta_{\nu,\nu'} \text{sgn}(x-x')$ where the suffix $-$ denotes the canonically conjugate variable. In terms of these phase variables, the field operator is expressed as

$$\psi_{p,\sigma,\mu}(x) = L^{-1/2} \sum_k e^{ikx} c_{k,p,\sigma,\mu} = \frac{1}{\sqrt{2\pi\alpha}} \exp(ipk_{F\mu}x + i\Theta_{p,\sigma,\mu}) \exp(i\pi\Xi_{p,\sigma,\mu}), \tag{2.6}$$

$$\Theta_{p,\sigma,\mu} = \frac{1}{2\sqrt{2}} [p\theta_{\rho+} + \theta_{\rho-} + \sigma(p\theta_{\sigma+} + \theta_{\sigma-}) + \mu(p\theta_{C+} + \theta_{C-}) + \sigma\mu(p\theta_{S+} + \theta_{S-})], \tag{2.7}$$

where α is of the order of the lattice constant. The phase factor $\pi\Xi_{p,\sigma,\mu}$ in Eq. (2.6), which is introduced for the anticommutation relation, is taken as

$$\Xi_{2n+j} = \hat{N}_1 + \cdots + \hat{N}_{2n} + \frac{(-1)^{j+1}}{2} (\hat{N}_{2n+1} + \hat{N}_{2n+2}), \tag{2.8}$$

where $j=1,2$ and $n=0,1,2,3$. The quantity \hat{N}_i denotes number operator, and the suffix i is related to (p,σ,μ) as, $(+,+,+)=1$, $(+,-,+)=2$, $(+,+,-)=3$, $(+,-,-)=4$, $(- ,+,+)=5$, $(-,-,+)=6$, $(-,+,-)=7$, and $(-,-,-)=8$, respectively. Such a choice of $\Xi_{p,\sigma,\mu}$ conserves a sign of interactions, which are represented by phase operators. In terms of these operators, Eq. (2.1) is rewritten as (Appendix A)

$$\begin{aligned}
\mathcal{H} = & \sum_{\nu=\rho,\sigma,C,S} \frac{v_\nu}{4\pi} \int dx \left[\frac{1}{K_\nu} (\partial\theta_{\nu+})^2 + K_\nu (\partial\theta_{\nu-})^2 \right] + \frac{g_\rho}{4\pi^2\alpha^2} \int dx \left[\cos\left(\sqrt{2}\theta_{C+} - \frac{4t}{v_F}x\right) + \cos\sqrt{2}\theta_{C-} \right] (\cos\sqrt{2}\theta_{S+} \\
& - \cos\sqrt{2}\theta_{S-}) + \frac{g_\sigma}{4\pi^2\alpha^2} \int dx \left[\cos\left(\sqrt{2}\theta_{C+} - \frac{4t}{v_F}x\right) - \cos\sqrt{2}\theta_{C-} \right] (\cos\sqrt{2}\theta_{S+} + \cos\sqrt{2}\theta_{S-}) \\
& + \frac{g_1}{2\pi^2\alpha^2} \int dx \cos\sqrt{2}\theta_{\sigma+} \left[\cos\left(\sqrt{2}\theta_{C+} - \frac{4t}{v_F}x\right) - \cos\sqrt{2}\theta_{C-} - \cos\sqrt{2}\theta_{S+} - \cos\sqrt{2}\theta_{S-} \right] \\
& + \frac{g_3}{2\pi^2\alpha^2} \int dx \cos\sqrt{2}\theta_{\rho+} \left[\cos\left(\sqrt{2}\theta_{C+} - \frac{4t}{v_F}x\right) + \cos\sqrt{2}\theta_{C-} - \cos\sqrt{2}\theta_{S+} + \cos\sqrt{2}\theta_{S-} \right], \tag{2.9}
\end{aligned}$$

where $v_\nu = v_F \sqrt{1 - (g_\nu/2\pi v_F)^2}$, $K_\nu = [(1 - g_\nu/2\pi v_F)/(1 + g_\nu/2\pi v_F)]^{1/2}$, $g_\rho = 2g_2 - g_1$, $g_\sigma = -g_1$, and $g_C = g_S = 0$.

We make use of the renormalization group method for response functions,²⁸⁻³⁰ which are assumed to be invariant for scaling $\alpha \rightarrow \alpha' = \alpha e^{dl}$. We express the nonlinear terms in Eq. (2.9) as $g_{\nu p, \nu' p'} / (2\pi^2\alpha^2) \int dx \cos\sqrt{2}\bar{\theta}_{\nu p} \cos\sqrt{2}\bar{\theta}_{\nu' p'}$, where $\sqrt{2}\bar{\theta}_{\nu p} = \sqrt{2}\theta_{\nu p} - 4tx/v_F$ for $\nu=C$ and $p=+$ and $\sqrt{2}\bar{\theta}_{\nu p} = \sqrt{2}\theta_{\nu p}$ otherwise. Then the coupling constants are given by $g_{C+,S+} = -g_{C-,S-} = (g_\rho + g_\sigma)/2$, $g_{C+,S-} = -g_{C-,S+} = (g_\rho - g_\sigma)/2$, $g_{\sigma+,C+} = -g_{\sigma+,C-} = -g_{\sigma+,S+} = -g_{\sigma+,S-} = g_1$, and $g_{\rho+,C+} = g_{\rho+,C-} = -g_{\rho+,S+} = g_{\rho+,S-} = g_3$. Response functions defined by $R_A(x_1 - x_2, \tau_1 - \tau_2) \equiv \langle T_\tau O_A(x_1, \tau_1) O_A^\dagger(x_2, \tau_2) \rangle$ are evaluated for SDW and SC states where τ_j is the imaginary time and O_A denotes the order parameter. Then renormalization group equations are expressed as²⁶ (Appendix B)

$$\begin{aligned}
\frac{d}{dl} K_\nu = & -\frac{1}{2\tilde{v}_\nu^2} K_\nu^2 [G_{\nu+,C+}^2 J_0(4\tilde{t}) + G_{\nu+,C-}^2 + G_{\nu+,S+}^2 \\
& + G_{\nu+,S-}^2], \tag{2.10}
\end{aligned}$$

$$\begin{aligned}
\frac{d}{dl} K_C = & \frac{1}{2} \sum_{p=\pm} \{ [-K_C^2 J_0(4\tilde{t}) \delta_{p,+} + \delta_{p,-}] \\
& \times (G_{\rho+,Cp}^2 + G_{\sigma+,Cp}^2 + G_{Cp,S+}^2 + G_{Cp,S-}^2) \}, \tag{2.11}
\end{aligned}$$

$$\begin{aligned}
\frac{d}{dl} K_S = & \frac{1}{2} \sum_{p=\pm} \{ (-K_S^2 \delta_{p,+} + \delta_{p,-}) \\
& \times [G_{\rho+,Sp}^2 + G_{\sigma+,Sp}^2 + G_{C+,Sp}^2 J_0(4\tilde{t}) + G_{C-,Sp}^2] \}, \tag{2.12}
\end{aligned}$$

$$\begin{aligned}
\frac{d}{dl} G_{\nu+,Cp} = & (2 - K_\nu - K_C^p) G_{\nu+,Cp} - G_{\nu+,S+} G_{Cp,S+} \\
& - G_{\nu+,S-} G_{Cp,S-}, \tag{2.13}
\end{aligned}$$

$$\begin{aligned}
\frac{d}{dl} G_{\nu+,Sp} = & (2 - K_\nu - K_S^p) G_{\nu+,Sp} - G_{\nu+,C+} G_{C+,Sp} J_0(4\tilde{t}) \\
& - G_{\nu+,C-} G_{C-,Sp}, \tag{2.14}
\end{aligned}$$

$$\begin{aligned}
\frac{d}{dl} G_{Cp,Sp} = & (2 - K_C^p - K_S^p) G_{Cp,Sp} - \frac{1}{\tilde{v}_\rho} G_{\rho+,Cp} G_{\rho+,Sp'} \\
& - \frac{1}{\tilde{v}_\sigma} G_{\sigma+,Cp} G_{\sigma+,Sp'}, \tag{2.15}
\end{aligned}$$

$$\begin{aligned}
\frac{d}{dl} \tilde{t} = & \tilde{t} - \frac{1}{4} K_C (G_{\rho+,C+}^2 + G_{\sigma+,C+}^2 + G_{C+,S+}^2 \\
& + G_{C+,S-}^2) J_1(4\tilde{t}), \tag{2.16}
\end{aligned}$$

where $\tilde{t}(l) = t(l)/\epsilon_F$, $\epsilon_F \equiv v_F \alpha^{-1}$, $\tilde{v}_\nu = v_\nu/v_F$, $\nu = \rho, \sigma$, and $p, p' = \pm$. In these equations, the l dependence is not written explicitly, and $J_n (n=0,1)$ is the n th order Bessel function.³¹ Initial conditions are given by $K_\nu(0) = K_\nu$, $G_{\nu p, \nu' p'}(0) = g_{\nu p, \nu' p'}/2\pi v_F$ and $\tilde{t}(0) = t/\epsilon_F$.

The second-order renormalization group equations with respect to all the coupling constants are derived by expanding as $K_\nu^{\pm 1}(l) = 1 \mp G_\nu(l) + \dots$. In case of $g_3 = 0$,¹⁹ these equations become equal to those of Fabrizio,¹² which satisfy the SU(2) symmetry with respect to spin rotation. Although such a symmetry is satisfied only approximately for Eqs. (2.10)–(2.12), the difference is very small within the present choice of parameters as is shown later. The renormalization equations of Eqs. (2.10)–(2.12) determine the fluctuations of the total charge, total spin, transverse charge, and transverse spin density, respectively. Equation (2.15) corresponds to forward scattering and backward scattering with parallel spins. In the right-hand side of these equations, there are bilinear terms with respect to $G_{\nu p, \nu' p'}(l)$, which appear in the presence of umklapp scattering and/or backward scattering while they are absent for only forward scattering. Equations (2.13) and (2.14) with $\nu = \rho (\nu = \sigma)$ correspond to umklapp scattering (backward scattering with opposite spins). It is found that there is a symmetry between equations of the total charge and those of the total spin, i.e., the renormalization equations remain the same for the replacement given by $K_\rho \leftrightarrow K_\sigma$, $v_\rho \leftrightarrow v_\sigma$, and

$$\begin{aligned}
& (G_{\rho+,C+}, G_{\rho+,C-}, G_{\rho+,S+}, G_{\rho+,S-}) \\
& \leftrightarrow (G_{\sigma+,C+}, G_{\sigma+,C-}, G_{\sigma+,S+}, G_{\sigma+,S-}).
\end{aligned}$$

Equation (2.16) is the scaling equation for the interchain hopping. It is noted that these equations with $t=0$ is reduced to those of a single chain.¹⁸

We examine order parameters for the possible states in case of repulsive interaction. In terms of phase variables, order parameters are expressed as (Appendix A)

$$\begin{aligned}
O_{\text{LSDW}_{\parallel,\text{out}}} &= \sum_{\sigma} \sigma (\psi_{+,\sigma,1}^{\dagger} \psi_{-,\sigma,1} - \psi_{+,\sigma,2}^{\dagger} \psi_{-,\sigma,2}) \\
&= \sum_{\sigma,\mu} \sigma \psi_{+,\sigma,\mu}^{\dagger} \psi_{-,\sigma,-\mu} \\
&\rightarrow e^{-i2k_F x} \sum_{\sigma} \exp[-i(\theta_{\rho+} + \sigma\theta_{\sigma+})/\sqrt{2}] \\
&\quad \times \cos[(\theta_{C-} + \sigma\theta_{S-})/\sqrt{2}], \quad (2.17)
\end{aligned}$$

$$\begin{aligned}
O_{\text{TSDW}_{\parallel,\text{out}}} &= \sum_{\sigma} (\psi_{+,-\sigma,1}^{\dagger} \psi_{-,-\sigma,1} - \psi_{+,\sigma,2}^{\dagger} \psi_{-,-\sigma,2}) \\
&= \sum_{\sigma,\mu} \psi_{+,\sigma,\mu}^{\dagger} \psi_{-,-\sigma,-\mu} \\
&\rightarrow e^{-i2k_F x} \sum_{\sigma} \sigma \exp[-i(\theta_{\rho+} + \sigma\theta_{\sigma-})/\sqrt{2}] \\
&\quad \times \sin[(\theta_{C-} + \sigma\theta_{S+})/\sqrt{2}], \quad (2.18)
\end{aligned}$$

$$\begin{aligned}
O_{\text{SS}_{\perp,\text{in}}} &= \sum_{\sigma} \sigma (\psi_{+,\sigma,1} \psi_{-,-\sigma,2} + \psi_{+,\sigma,2} \psi_{-,-\sigma,1}) \\
&= \sum_{\sigma,\mu} \sigma \mu \psi_{+,\sigma,\mu} \psi_{-,-\sigma,\mu} \\
&\rightarrow \sum_{\sigma} \sigma \exp[i(\theta_{\rho-} + \sigma\theta_{\sigma+})/\sqrt{2}] \\
&\quad \times \sin[(\theta_{C-} + \sigma\theta_{S+})/\sqrt{2}], \quad (2.19)
\end{aligned}$$

where $\psi_{p,\sigma,i}(x) = (1/\sqrt{L}) \sum_k e^{ikx} a_{k,p,\sigma,i}$. In Eqs. (2.17)–(2.19), $\text{LSDW}_{\parallel,\text{out}}$ ($\text{TSDW}_{\parallel,\text{out}}$) denotes longitudinal (transverse) SDW with intrachain and out-of-phase pairing. The suffix $\text{SS}_{\perp,\text{in}}$ represents the SCd state, i.e., the singlet SC state with interchain and in-phase pairing.

The renormalization group technique is also applied to the calculation of response functions for the order parameters, Eqs. (2.17)–(2.19). Normalized response functions are derived as (Appendix B)

$$\begin{aligned}
\bar{R}_{\text{LSDW}_{\parallel,\text{out}}}(r) &= \exp\left(\int_0^{\ln(r/\alpha)} dl \left\{ -\frac{1}{2} [K_{\rho}(l) + K_{\sigma}(l) \right. \right. \\
&\quad \left. \left. + 1/K_C(l) + 1/K_S(l)] - G_{C-,S-}(l) \right. \right. \\
&\quad \left. \left. - G_{\sigma+,C-}(l) - G_{\sigma+,S-}(l) \right\} \right), \quad (2.20)
\end{aligned}$$

$$\begin{aligned}
\bar{R}_{\text{TSDW}_{\parallel,\text{out}}}(r) &= \exp\left(\int_0^{\ln(r/\alpha)} dl \left\{ -\frac{1}{2} [K_{\rho}(l) + 1/K_{\sigma}(l) \right. \right. \\
&\quad \left. \left. + 1/K_C(l) + K_S(l)] + G_{C-,S+}(l) \right\} \right), \quad (2.21)
\end{aligned}$$

$$\begin{aligned}
\bar{R}_{\text{SS}_{\perp,\text{in}}}(r) &= \exp\left(\int_0^{\ln(r/\alpha)} dl \left\{ -\frac{1}{2} [1/K_{\rho}(l) + K_{\sigma}(l) + 1/K_C(l) \right. \right. \\
&\quad \left. \left. + K_S(l)] + G_{C-,S+}(l) - G_{\sigma+,C-}(l) \right. \right. \\
&\quad \left. \left. + G_{\sigma+,S+}(l) \right\} \right), \quad (2.22)
\end{aligned}$$

where $r = [x^2 + (v_F \tau)^2]^{1/2}$ and the quantities $K_{\nu}(l)$ ($\nu = \rho, \sigma, C$, and S) and $G_{\nu p, \nu' p'}(l)$ ($p, p' = \pm$) are calculated from Eqs. (2.10)–(2.15). In these equations, the renormalization of the velocity²⁸ has been discarded in a way similar to the spinless case.³⁰

III. CONFINEMENT VS DECONFINEMENT

We examine confinement-deconfinement transition by calculating the renormalization group equations for interactions of both the Hubbard model and the general model with $g_1 \neq g_2$. The scaling quantity $l (= \ln r/\alpha)$ is related to energy ω and/or temperature T by the relation that $l = \ln(\epsilon_F/\omega) = \ln(\epsilon_F/T)$. Numerical calculation is performed by use of normalized quantities $\tilde{g}_j \equiv g_j/(2\pi v_F)$ for $j = 1 \sim 3$.

In Fig. 1(a), quantities $\tilde{t}(l)$ and $1/K_C(l)$ as a function of l are shown by solid curves and dashed curves, respectively, with the fixed $\tilde{g}_3 = 0.05$, $\tilde{g}_{3c} (= 0.119)$ and 0.3 where $t/\epsilon_F = 0.1$, and $\tilde{g}_1 = \tilde{g}_2 = 0.4$. Both mutual interactions and umklapp scattering suppress the increase of $\tilde{t}(l)$ as is seen from Eq. (2.16). In the case of $\tilde{g}_3 = 0.05$, $\tilde{t}(l)$ [solid curve (I)] increases rapidly. Such a behavior of $\tilde{t}(l)$ denotes the deconfinement of the transverse hopping. The corresponding $1/K_C(l)$ shown by dashed curve (I) decreases monotonically to zero indicating a formation of the transverse charge gap. In the present case, some of $G_{\nu p, \nu' p'}(l)$ diverge at finite l and then solutions stop due to the second-order renormalization group equations. It is expected that the calculation with third-order equations gives the finite value of $G_{\nu p, \nu' p'}(l)$ for all values of l .¹² A noticeable difference appears for large value of the umklapp scattering as is shown for $\tilde{g}_3 = 0.3$ [curves (3) and (III)]. With increasing l , $\tilde{t}(l)$ [curve (3)] takes a maximum and reduces to zero and $1/K_C(l)$ [curve (III)] remains finite even at the limiting value of l . Such a behavior of $\tilde{t}(l)$ indicates the absence of interchain hopping, which leads to confinement of electrons within a single chain. There is no transverse charge gap due to finite $K_C(l)$, where the oscillatory behavior comes from the Bessel functions in Eqs. (2.10)–(2.15) obtained with use of the sharp cutoff in the formulation of renormalization group technique.²⁸ The fact that

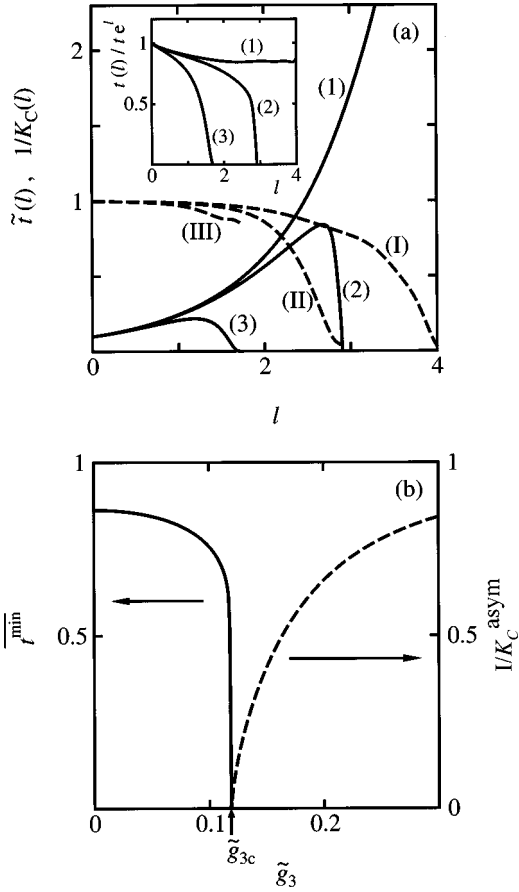


FIG. 1. (a) The l -dependences of $\tilde{t}(l)$ (solid curves) and $1/K_C(l)$ (dashed curves) for $\tilde{g}_3 = 0.05$ [(1) and (I)], $\tilde{g}_3 = \tilde{g}_{3c} (=0.119)$ [(2) and (II)], and $\tilde{g}_3 = 0.3$ [(3) and (III)], respectively, where $t/\epsilon_F = 0.1$ and $\tilde{g}_1 = \tilde{g}_2 = 0.4$. In the inset, curves (1), (2), and (3) denote $t(l)/te^l$ for $\tilde{g}_3 = 0.05$ (1), \tilde{g}_{3c} (2), and 0.3 (3). (b) The \tilde{g}_3 -dependences of \tilde{t}^{\min} and $1/K_C^{\text{asym}}$. The quantity \tilde{t}^{\min} denotes a minimum of $t(l)/te^l$ and the quantity $1/K_C^{\text{asym}}$ is the limiting value of $1/K_C(l)$. The arrow denotes the critical value $\tilde{g}_3 = \tilde{g}_{3c}$ corresponding to a boundary between deconfinement and confinement.

$$\begin{aligned}
 G_{\rho+,c+}(l)/G_{\rho+,c-}(l) & \\
 & \simeq G_{\sigma+,c+}(l)/G_{\sigma+,c-}(l) \\
 & \simeq G_{c+,s+}(l)/G_{c-,s+}(l) \\
 & \simeq G_{c+,s-}(l)/G_{c-,s-}(l) \simeq 1/K_C(l)
 \end{aligned}$$

for the limiting value is consistent with the irrelevance of the interchain hopping. At a critical value given by $\tilde{g}_3 = \tilde{g}_{3c}$, a transition from deconfinement to confinement takes place where both $\tilde{t}(l)$ and $1/K_C(l)$ reduce to zero at the limiting value of l [curves (2) and (II)]. In the inset, the normalized interchain hopping, $t(l)/te^l$, is shown for $\tilde{g}_3 = 0.1$ (1), 0.119 (2), and 0.3 (3), where te^l denotes the value for the noninteracting one. The limiting behavior of curve (1), which remains constant for large l , indicates deconfinement. In Fig. 1(b), the \tilde{g}_3 dependences of $1/K_C^{\text{asym}}$ and \tilde{t}^{\min} are shown where $1/K_C^{\text{asym}}$ is the limiting value of $1/K_C$. The quantity \tilde{t}^{\min} denotes a minimum of $t(l)/te^l$, which is found

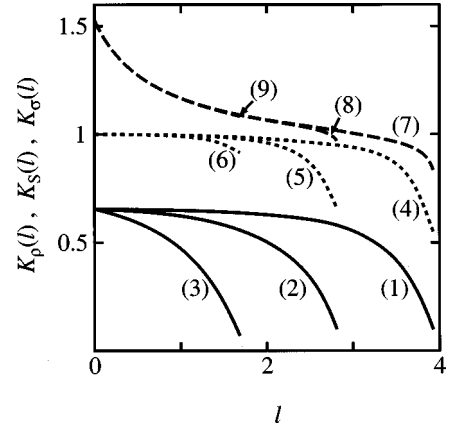


FIG. 2. The l -dependences of $K_\rho(l)$, $K_S(l)$, and $K_\sigma(l)$ are shown by solid curves, dotted curves, and dashed curves for $\tilde{g}_3 = 0.05$ [(1), (4), (7)], \tilde{g}_{3c} [(2), (5), (8)], and 0.3 [(3), (6), (9)], respectively, where parameters are the same as those in Fig. 1(a).

with increasing l from zero [e.g., curve (1) in the inset of Fig. 1(a)], and is essentially the same as the limiting value. Deconfinement is obtained for finite \tilde{t}^{\min} while confinement is found for finite $1/K_C^{\text{asym}}$. Both \tilde{t}^{\min} and $1/K_C^{\text{asym}}$ are reduced to zero at $\tilde{g}_3 = \tilde{g}_{3c}$, which denotes a critical value for deconfinement-confinement transition. We note that the Bessel function $J_1[4\tilde{t}(l)]$ in Eq. (2.16) is crucial to obtain such a transition. Actually, in the right-hand side of Eq. (2.16), the second term becomes negligible for deconfinement, but the second term becomes larger than the first term for confinement.

In Fig. 2, the corresponding l dependences for $K_\rho(l)$, $K_\sigma(l)$, and $K_S(l)$ are shown by solid curves, dotted curves, and dashed curves, respectively, where numerical results are shown for $|G_{\nu\rho, \nu'\rho'}(l)| < 10$. Curves (1), (4), and (7) are for $\tilde{g}_3 = 0.05$, curves (2), (5), and (8) are for $\tilde{g}_3 = \tilde{g}_{3c}$, and curves (3), (6), and (9) are for $\tilde{g}_3 = 0.3$. The quantity $K_\rho(l)$ as a function of l decreases to zero. A charge gap is formed for $K_\rho(l) \simeq K_\rho/2$, which gives a result consistent with that of the Hubbard model.³² The transverse spin fluctuation is also suppressed by umklapp scattering because $K_S(l)$ with the fixed l is reduced by \tilde{g}_3 . However, the \tilde{g}_3 dependence of $K_\sigma(l)$ is very small, i.e., the l dependence of $K_\sigma(l)$ is similar to the one-dimensional case. Therefore, there is no behavior of spin gap for the total spin fluctuation except for very low energy. We note that, for single chain, $K_\sigma(l)$ decreases monotonically to $K_\sigma(l \rightarrow \infty) \rightarrow 1$ and that $K_S(l) = 1$ for all l . From these l dependences, it is found that a separation of freedoms of charge and spin still exists at energy corresponding to the formation of the charge gap.

In Fig. 3, the t dependence of \tilde{g}_{3c} is shown for $\tilde{g}_1 = \tilde{g}_2 \equiv \tilde{g} = 0, 0.2, \text{ and } 0.4$ where confinement (deconfinement) is obtained for $\tilde{g} > \tilde{g}_{3c}$ ($\tilde{g} < \tilde{g}_{3c}$). The \tilde{g}_{3c} dependence of t for $\tilde{g} = 0$ is expressed as

$$t/\epsilon_f \simeq K_1 \exp(-\pi/4\tilde{g}_3), \quad (3.1)$$

where $K_1 \simeq 1.2$. The intrachain interaction enhances the confined region. The presence of \tilde{g} leads to a different behavior

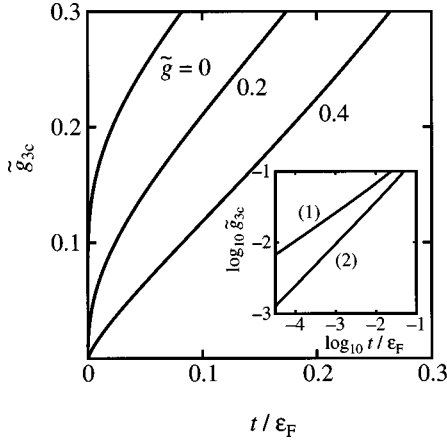


FIG. 3. The critical value \tilde{g}_{3c} are shown as the function of t/ϵ_F for $\tilde{g}=0, 0.2$, and 0.4 , where confinement (deconfinement) is obtained for $\tilde{g}_3 > \tilde{g}_{3c}$ ($\tilde{g}_3 < \tilde{g}_{3c}$). In the inset, the $\log t/\epsilon_F - \log \tilde{g}_{3c}$ plot is shown for $\tilde{g}=0.2$ (1) and 0.3 (2).

for t with small \tilde{g}_3 . From the inset, which is calculated for $\tilde{g}=0.2$ (1) and 0.3 (2), it turns out that the \tilde{g}_{3c} dependence of t for $\tilde{g} \neq 0$ is obtained as

$$t/\epsilon_F \approx K_2 (\tilde{g}_{3c}/K_3)^{1/2\tilde{g}}, \quad (3.2)$$

where $K_2 \approx 0.2$, $K_3 \approx 0.2$, and $\tilde{g}_{3c} \ll 1$. The range of \tilde{g}_{3c} , in which Eq. (3.2) is valid, decreases with decreasing \tilde{g} , e.g., the upper bound of \tilde{g}_{3c} is given by 0.15 , 0.04 , and 0 for $\tilde{g}=0.4, 0.2$, and 0 , respectively. Coefficients K_1 , K_2 , and K_3 have been derived numerically since analytical treatment is very complicated. We note that the magnitude of \tilde{g}_{3c} is determined mainly by the balance between the charge gap created by the umklapp scattering and the energy of interchain hopping as is shown later. As t goes to zero, \tilde{g}_{3c} reduces to zero and then the interchain hopping becomes always relevant in the absence of umklapp scattering within the present choice of intrachain interaction.

Now we examine the boundary between confinement and deconfinement as the function of \tilde{g}_1 and \tilde{g}_2 with the fixed t . From the calculation with some choices of $t/\epsilon_F=0.1$, we find it a good approximation that the boundary with fixed \tilde{g}_3 depends only on $2\tilde{g}_2 - \tilde{g}_1$. Therefore, \tilde{g}_{3c} is determined essentially as the function of $2\tilde{g}_2 - \tilde{g}_1$, i.e., K_ρ . Such a result originates in the fact that the $G_{\rho+, C+}(l)$ term gives a dominant contribution and the effect of g_σ is negligibly small for other coupling constants in the right-hand side of Eq. (2.16). In Fig. 4, the quantity \tilde{g}_{3c} as the function of $2\tilde{g}_2 - \tilde{g}_1$ is shown by the solid curves with choices of $t/\epsilon_F=0.1$ and 0.01 , where $\tilde{g}_1=0.2$. The region of $\tilde{g}_3 > \tilde{g}_{3c}$ ($\tilde{g}_3 < \tilde{g}_{3c}$) corresponds to the confinement (deconfinement). The dotted curve is explained in Sec. IV. With increasing $2\tilde{g}_2 - \tilde{g}_1$ (i.e., decreasing K_ρ), the region for the confinement is enhanced.

By use of response functions for order parameters [Eqs. (2.17)–(2.19)], we calculate states at finite temperatures where a crossover is shown on the plane of \tilde{g}_3 and normalized temperature T/ϵ_F (or energy) in Fig. 5. The dotted curve denotes the temperature corresponding to the gap for the to-

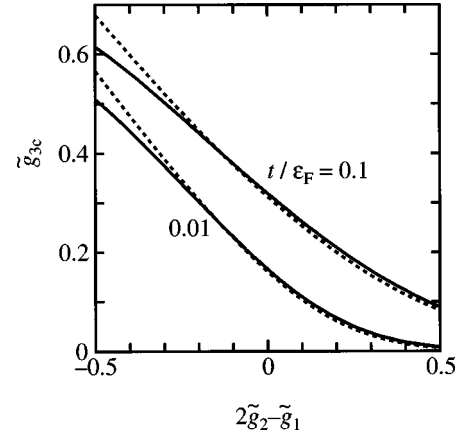


FIG. 4. The critical values \tilde{g}_{3c} as the function of $2\tilde{g}_2 - \tilde{g}_1$ for $t/\epsilon_F=0.1$ and 0.01 with the fixed $\tilde{g}_1=0.2$. The solid curves denote the boundaries obtained for Eqs. (2.10)–(2.16), while the dotted curves are obtained in terms of the expanded K_ρ .

tal charge Δ , where $\Delta \equiv \epsilon_F \exp[-l_g]$ and $K_\rho(l_g) \equiv K_\rho/2$. Around the energy corresponding to the charge gap, the total spin shows a behavior similar to the one-dimensional case with the gapless excitation. The solid curve, which is obtained from $\epsilon_F \exp[-l_g]$ with $\tilde{t}(l_g)=1$ denotes the crossover temperature, below which the state reveals the property of two-coupled chains. Such a temperature becomes lower than the bare interchain hopping energy $t/\epsilon_F=0.1$ due to the renormalization by the intrachain interaction.^{10,30} The dash-dotted line denotes a boundary where the decrease of temperature leads to confinement (deconfinement) for $\tilde{g}_3 > \tilde{g}_{3c}$ ($\tilde{g}_3 < \tilde{g}_{3c}$). One finds the following four kinds of regions (I)–(IV), which are separated by these boundaries. The dominant state in region (I) is one-dimensional SDW. In region (II), interchain hopping removes the degeneracy of the out-of-phase state and the in-phase state,³⁰ but the energy

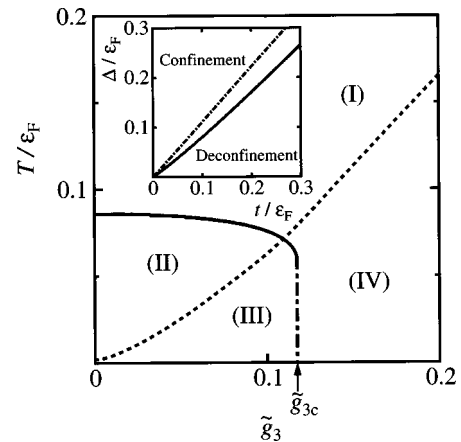


FIG. 5. A crossover is shown on the plane of \tilde{g}_3 and temperature T/ϵ_F (or energy) where $t/\epsilon_F=0.1$ and $\tilde{g}_1=\tilde{g}_2=0.4$. The dotted curve and solid curve denote $\Delta (\equiv \epsilon_F \exp[-l_g])$ and $\epsilon_F e^{-l}$, respectively, where $K_\rho(l_g)=K_\rho/2$ and $\tilde{t}(l_g)=1$. The dash-dotted line separates the region of confinement from that of deconfinement. In the inset, the phase diagram of confinement and deconfinement is shown on the plane of t/ϵ_F and Δ/ϵ_F where the dash-dotted (solid) curve denotes the boundary for $\tilde{g}=0$ (0.4).

is still high compared with the gaps for the transverse fluctuations, which develop just above Δ (dotted curve). In this region, one finds a crossover into the out-of-phase SDW state. The present calculation indicates a short-range correlation for the SCd state in a certain domain with small \tilde{g}_3 (<0.001) and finite temperatures just above the dotted curve. This could retain a trace that the ground state for $\tilde{g}_3 = 0$ is given by the SC state.^{12,16,17} In region (III), the gap of the total charge fluctuation develops. At very low temperatures, all the fluctuations become gapful due to relevant interchain hopping. In this case, the correlation of the SCd state as well as the SDW state decays exponentially. We note that such a state in the limit of low energy corresponds to the ‘‘COSO’’ phase, which has been obtained at half-filled band by Balents and Fisher.¹⁷ In region (IV), the gap of the total charge is so large that the interchain hopping becomes irrelevant leading to the isolated chains²⁴ and then the absence of other gaps. The state in this region has a resemblance to that of the half-filled one-dimensional chain.¹⁸ In the inset, we show a phase diagram of confinement and deconfinement on the plane of t/ϵ_F and Δ/ϵ_F in the limit of absolute zero temperature, where the dash-dotted curve (solid curve) corresponds to $\tilde{g}=0$ (0.4) in Fig. 3. The region for confinement increases by the increase of intrachain interaction \tilde{g} . The ratio in the interval region of $0.01 < t/\epsilon_F < 0.3$ is given by $\Delta/t \approx 1.1$ ($0.7 < \Delta/t < 0.9$) for $\tilde{g}=0$ (0.4).³¹ These results indicate the fact that the deconfinement-confinement transition is determined essentially by the competition between the charge gap and the interchain hopping energy.

IV. DISCUSSION

In the present paper, the effect of umklapp scattering on two-coupled chains has been examined by calculating the boundary for confinement and deconfinement as the function of umklapp scattering, interchain hopping, and intrachain interactions. It has been shown that electrons are confined in a single chain when interchain hopping becomes smaller than a critical value of the order of the charge gap or the umklapp scattering exceeds a threshold.

We discuss the validity of our calculation of renormalization group equations given by Eqs. (2.10)–(2.16). Here we calculate these equations by making use of the expansion, $K_\nu^{\pm 1}(l) = 1 \mp G_\nu(l) + \dots$ ($\nu = \rho, \sigma, C$, and S), where the initial conditions are $G_\nu(0) = g_\nu/2\pi v_F$. Since such a method leads to a solution with the SU(2) symmetry, we have done the following two kinds of evaluations. One of them is shown in Fig. 4 by the dotted curve, which denotes \tilde{g}_{3c} as a function of intrachain interaction with fixed $t/\epsilon_F = 0.1$ and 0.01. A good coincidence between the solid curve and the dotted curve is obtained for $2\tilde{g}_2 - \tilde{g}_1 > 0$. The other is shown in Fig. 6 by the dotted curve, which denotes \tilde{g}_{3c} as a function of t/ϵ_F for $\tilde{g}_1 = \tilde{g}_2 = \tilde{g} = 0.3$. There is a small difference between the result without the expansion of K_ν (solid curve) and that with the expansion of K_ν . Thus, such a calculation may be justified within the present choice of parameters.

Instead of treating two-coupled chains with the split Fermi surface, Khveshchenko and Rice applied the bosonization method to two degenerate bands and enlarged the pa-

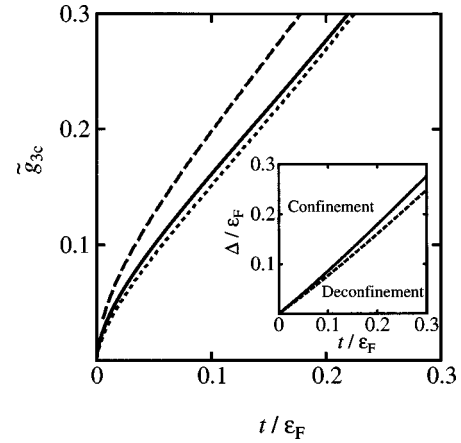


FIG. 6. The critical value \tilde{g}_{3c} as the function of t/ϵ_F for $\tilde{g} = 0.3$. The solid curve corresponds to the calculation in Fig. 3 and the dotted curve is obtained by use of the expanded K_ν . The dashed curve is the results for $\tilde{g}_1 = \tilde{g}_2 = \tilde{g}_4 = 0.3$. In the inset, the phase diagram of confinement and deconfinement is shown on the plane of t/ϵ_F and Δ/ϵ_F for $\tilde{g}_1 = \tilde{g}_2 = 0.3$ where the solid (dashed) curve is calculated for $\tilde{g}_4 = 0$ ($\tilde{g}_4 = 0.3$).

rameter space of the renormalization group to examine the pair hopping for the case of the relevant interchain hopping.¹⁵ We discuss the effect of the pair-hopping process on the present result with the half-filled band. Expressing the pair hopping in terms of Eqs. (2.2)–(2.5), we obtain nonlinear terms consisting of $\theta_{\rho+}, \theta_{\sigma+}, \theta_{C+}$ and θ_{S+} , which are also found in Eq. (2.9), except for a new term given by $g_8 \cos(\sqrt{2}\theta_{\rho+}) \cos(\sqrt{2}\theta_{\sigma+})$.¹⁵ When the interchain hopping is larger than the charge gap, the pair hopping becomes relevant. In such a region, $\tilde{t}(l)$ and $K_\rho(l)$ of the present paper exhibit trajectories similar to those of Ref. 15 and the differences in magnitudes are small, although the g_8 term gives rise to a visible enhancement of the spin gap obtained by $K_\sigma(l)$. It is noted that the interchain hopping is not renormalized directly by the g_8 term since the right-hand side of Eq. (2.16) is determined only by terms including θ_{C+} . When the interchain hopping is smaller than the charge gap, the pair hopping becomes irrelevant due to confinement, e.g., $g_8 \approx 0$ at the energy of the charge gap. Therefore, it is considered that the effect of the pair hopping is small for the boundary between confinement and deconfinement.

Now we examine the effect of the forward scattering with the same branch, where the coupling constant is given by g_4 . The Hamiltonian corresponding to g_4 is expressed as

$$\mathcal{H}_{\text{int}}^{g_4} \equiv \frac{g_4}{2L} \sum_{p,\sigma,i} \sum_{k_1,k_2,q} a_{k_1,p,\sigma,i}^\dagger a_{k_2,p,-\sigma,i}^\dagger \times a_{k_2+q,p,-\sigma,i} a_{k_1-q,p,\sigma,i}, \quad (4.1)$$

which has two kinds effects. One of them appears in K_ρ , K_σ , v_ρ , and v_σ , which are written as $K_\rho = \{[1 - \tilde{g}_\rho / (1 + \tilde{g}_4)] / [1 + \tilde{g}_\rho / (1 + \tilde{g}_4)]\}^{1/2}$, $K_\sigma = \{[1 - \tilde{g}_\sigma / (1 - \tilde{g}_4)] / [1 + \tilde{g}_\sigma / (1 - \tilde{g}_4)]\}^{1/2}$, $v_\rho = v_F [(1 + \tilde{g}_4)^2 - \tilde{g}_\rho^2]^{1/2}$, and $v_\sigma = v_F [(1 - \tilde{g}_4)^2 - \tilde{g}_\sigma^2]^{1/2}$ with $\tilde{g}_\nu = g_\nu / 2\pi v_F$. Another is the nonlinear terms given by

$$\frac{1}{2\pi^2\alpha^2} \int dx \left[g_{C+,C-} \cos\left(\sqrt{2}\theta_{C+} - \frac{4t}{v_F}x\right) \times \cos\sqrt{2}\theta_{C-} + g_{S+,S-} \cos\sqrt{2}\theta_{S+} \cos\sqrt{2}\theta_{S-} \right], \quad (4.2)$$

where $g_{C+,C-} = -g_{S+,S-} = g_4$. Equation (4.2) leads to additional terms to renormalization group equations for $\tilde{t}(l)$ and $K_C(l)$, which are of the order of $o(\tilde{t}^3)$ and $o(\tilde{t}^4)$, respectively. There is also renormalization for $G_{C+,C-}$ and $G_{S+,S-}$. However, we found that, in the present calculation, the latter effect given by Eq. (4.2) is negligibly small. On the other hand, in the former case, there is a noticeable effect of g_4 , which comes from the variation of K_ρ . Note that $K_\rho (<1)$ increases with increasing \tilde{g}_4 since the effect of g_4 is equivalent to replacing \tilde{g}_ρ by $\tilde{g}_\rho/(1+\tilde{g}_4)$ in K_ρ . The increase of $K_\rho (<1)$ reduces the renormalization of umklapp scattering $G_{\rho+,C+}$. Then one needs larger \tilde{g}_3 to obtain the confinement. An example with $\tilde{g}=0.3$ is shown in Fig. 6 where \tilde{g}_{3c} including the \tilde{g}_4 term (dashed curve) is compared with that with $\tilde{g}_4=0$ (solid curve). The quantity \tilde{g}_{3c} is increased by g_4 , i.e., the suppression of the region of the confinement on the plane of t/ϵ_F and \tilde{g}_3 . In the inset, a phase diagram of confinement and deconfinement is shown on the plane of t/ϵ_F and Δ/ϵ_F for both $\tilde{g}_4=0$ (solid curve) and $\tilde{g}_4 \neq 0$ (dashed curve). The fact that the critical value of Δ is reduced by g_4 is understood as follows. The magnitude of $K_\rho(0)$ for $\tilde{g}_4 \neq 0$ is larger than that for $\tilde{g}_4=0$, although the difference between these two cases is very small as for the right-hand side of Eq. (2.10). Since larger $K_\rho(0)$ leads to

slower decrease of $K_\rho(l)$, one obtains smaller gap Δ in the presence of g_4 . Thus, it is found that g_4 reduces the effects of both intrachain interaction and umklapp scattering.

Based on the present calculation, we comment on electronic states for TMTSF and TMTTF salts, both of which show the correlation gap above the SDW state. Such a gap is possible for a choice of $T/\epsilon_F \approx 10^{-2}$ in Fig. 5 where $\epsilon_F \approx 10^3$ K and $T \approx 10$ K.¹ The fact that the plasma edge perpendicular to chains is present for TMTSF salt (absent for TMTTF salt)⁸ suggests the relevance (irrelevance) of the interchain hopping. These behaviors of interchain hopping are found when the umklapp scattering satisfies $\tilde{g}_3 \lesssim \tilde{g}_{3c}$ for TMTSF salt and $\tilde{g}_3 \gtrsim \tilde{g}_{3c}$ for the TMTTF salt. Thus, the existence of dimerization, which increases \tilde{g}_3 , is crucial to understand property of these salts above the SDW state.

For the metallic state, the above organic conductors may be regarded as a doped system rather half filling since one-particle hopping between chains leads to a small deviation from the commensurate one.²⁴ In this case, the metallic state is expected with increasing the doping rate as is shown in a one-dimensional case.³³ Actually, a crossover from confinement to deconfinement has been obtained in the presence of doping even for two-coupled chains.³⁴ It will be of interest to study such an effect of doping on many-coupled chains.

ACKNOWLEDGMENTS

The authors thank G. Grüner and H. Yoshioka for useful discussions. This paper was partially supported by a Grant-in-Aid for Scientific Research from the Ministry of Education, Science, Sports and Culture (Grant No. 09640429), Japan.

APPENDIX A: PHASE REPRESENTATION OF \mathcal{H} AND ORDER PARAMETERS

By making use of $a_{k,p,\sigma,i} = [(-1)^i c_{k,p,\sigma,+} + c_{k,p,\sigma,-}]$ ($i=1,2$) and $\psi_{p,\sigma,\mu}(x) = L^{-1/2} \sum_k e^{ikx} c_{k,p,\sigma,\mu}$, Eq. (2.1) is rewritten in terms of $\psi_{p,\sigma,\mu}$. The terms for interactions are divided into two parts, which consist of the scattering between electrons with same μ and the scattering between electrons with opposite μ . since the former part is treated in the way similar to the kinetic energy, we examine the latter part, which is defined as \mathcal{H}_{int} . By defining $\psi'_{p,\sigma,\mu}$ as $\psi'_{p,\sigma,\mu}(x) = (1/\sqrt{2\pi\alpha}) \exp(ipk_F \mu x + i\Theta_{p,\sigma,\mu})$, \mathcal{H}_{int} is written as

$$\begin{aligned} \mathcal{H}_{\text{int}} = & \frac{1}{4} \sum_{p,\sigma,\mu} \int dx \{ g_1 \psi'_{p,\sigma,\mu} \psi'_{-p,\sigma,\mu} \psi'_{p,\sigma,-\mu} \psi'_{-p,\sigma,-\mu} e^{i(\sigma\mu)2\pi\hat{N}_a} + g_1 \psi'_{p,\sigma,\mu} \psi'_{-p,-\sigma,\mu} \psi'_{p,-\sigma,-\mu} \psi'_{-p,-\sigma,-\mu} e^{i(p\sigma)2\pi\hat{N}_d + i\pi} \\ & + g_1 \psi'_{p,\sigma,\mu} \psi'_{-p,\sigma,-\mu} \psi'_{p,\sigma,-\mu} \psi'_{-p,\sigma,\mu} e^{i(p\sigma\mu)2\pi\hat{N}_b + i\pi} + g_1 \psi'_{p,\sigma,\mu} \psi'_{-p,-\sigma,-\mu} \psi'_{p,-\sigma,-\mu} \psi'_{-p,\sigma,\mu} e^{i(p\sigma)2\pi\hat{N}_d} \\ & + g_1 \psi'_{p,\sigma,\mu} \psi'_{-p,-\sigma,\mu} \psi'_{p,-\sigma,\mu} \psi'_{-p,\sigma,\mu} e^{-i(p\sigma)2\pi[\hat{N}_b + \mu\hat{N}_d] + i\pi} \\ & + g_1 \psi'_{p,\sigma,\mu} \psi'_{-p,-\sigma,-\mu} \psi'_{p,-\sigma,\mu} \psi'_{-p,\sigma,-\mu} e^{-i(p\sigma)2\pi[\hat{N}_b + p\mu\hat{N}_c] + i\pi} + g_2 \psi'_{p,\sigma,\mu} \psi'_{-p,\sigma,-\mu} \psi'_{p,\sigma,\mu} \psi'_{-p,\sigma,-\mu} e^{i(p\sigma\mu)2\pi\hat{N}_b} \\ & + g_2 \psi'_{p,\sigma,\mu} \psi'_{-p,-\sigma,-\mu} \psi'_{p,-\sigma,\mu} \psi'_{-p,\sigma,-\mu} e^{i(\sigma\mu)2\pi\hat{N}_a + i\pi} + g_2 \psi'_{p,\sigma,\mu} \psi'_{-p,\sigma,\mu} \psi'_{p,-\sigma,-\mu} \psi'_{-p,\sigma,-\mu} e^{i(\sigma\mu)2\pi\hat{N}_a + i\pi} \\ & + g_2 \psi'_{p,\sigma,\mu} \psi'_{-p,-\sigma,\mu} \psi'_{p,-\sigma,-\mu} \psi'_{-p,\sigma,-\mu} e^{i(p\sigma\mu)2\pi\hat{N}_b} + g_3 e^{ip4k_F x} \psi'_{p,\sigma,\mu} \psi'_{p,-\sigma,\mu} \psi'_{-p,-\sigma,\mu} \psi'_{-p,\sigma,\mu} e^{ip4\pi[\hat{N}_a + \delta_{\mu,+}\hat{N}_b - \delta_{\mu,-}\hat{N}_d]} \\ & + g_3 e^{ip4k_F x} \psi'_{p,\sigma,\mu} \psi'_{p,-\sigma,-\mu} \psi'_{-p,-\sigma,-\mu} \psi'_{-p,\sigma,\mu} e^{i(p\sigma\mu)2\pi\hat{N}_b + i\pi} + g_3 e^{ip4k_F x} \psi'_{p,\sigma,\mu} \psi'_{p,-\sigma,-\mu} \psi'_{-p,-\sigma,-\mu} \psi'_{-p,\sigma,-\mu} e^{i(\sigma\mu)2\pi\hat{N}_a} \\ & + g_3 e^{ip4k_F x} \psi'_{p,\sigma,\mu} \psi'_{p,-\sigma,\mu} \psi'_{-p,-\sigma,-\mu} \psi'_{-p,\sigma,-\mu} e^{ip2\pi[\delta_{p,\mu,+}(\hat{N}_a - \hat{N}_7 - \hat{N}_8) + \delta_{p,\mu,-}(\hat{N}_3 + \hat{N}_4)]} \}, \end{aligned} \quad (A1)$$

where $\hat{N}_a = [(\hat{N}_1 + \hat{N}_2) + (\hat{N}_3 + \hat{N}_4) + (\hat{N}_5 + \hat{N}_6) + (\hat{N}_7 + \hat{N}_8)]/4$, $\hat{N}_b = [\{(\hat{N}_1 + \hat{N}_2) + (\hat{N}_3 + \hat{N}_4)\} - \{(\hat{N}_5 + \hat{N}_6) + (\hat{N}_7 + \hat{N}_8)\}]/4$, $\hat{N}_c = [\{(\hat{N}_1 + \hat{N}_2) - (\hat{N}_3 + \hat{N}_4)\} + \{(\hat{N}_5 + \hat{N}_6) - (\hat{N}_7 + \hat{N}_8)\}]/4$ and $\hat{N}_d = [\{(\hat{N}_1 + \hat{N}_2) - (\hat{N}_3 + \hat{N}_4)\} - \{(\hat{N}_5 + \hat{N}_6) - (\hat{N}_7 + \hat{N}_8)\}]/4$. By defining N_i as the eigenvalue of \hat{N}_i , it is found that the factor in Eq. (A1) commutes with the Hamiltonian, Eq. (2.1), when N_a, N_b, N_c , and N_d are integers. Such a choice of Hilbert space leads to negative sign for 2, 3, 5, 6, 8, 9, and 12th terms in Eq. (A1). By expressing $\psi'_{p,\sigma,\mu}(x)$ in terms of the phase variables, we obtain the nonlinear terms in Eq. (2.9).

Next we examine order parameters. For order parameter $O_{\text{LSDW}_{\parallel,\text{out}}}$, which is expressed as $O_{\text{LSDW}_{\parallel,\text{out}}} = -\sum_{\sigma,\mu} \sigma \psi_{+,\sigma,\mu}^\dagger \psi_{-,\sigma,-\mu} = -(\psi_1^\dagger \psi_7 + \psi_3^\dagger \psi_5) + (\psi_2^\dagger \psi_8 + \psi_4^\dagger \psi_6)$, we evaluate the correlation function given by $\langle O_{\text{LSDW}_{\parallel,\text{out}}}(x) O_{\text{LSDW}_{\parallel,\text{out}}}^\dagger(0) \rangle$. By noting that a typical term of this correlation function is rewritten as

$$\begin{aligned} \langle [\psi_1^\dagger(x) \psi_7(x)] [\psi_2^\dagger(0) \psi_8(0)]^\dagger \rangle &= \langle \psi_1^\dagger(x) \psi_7'(x) \psi_8^\dagger(0) \psi_2'(0) e^{-i2\pi[\hat{N}_b + \hat{N}_c] + i\pi} \rangle \\ &= -\langle [\psi_1^\dagger(x) \psi_7'(x)] [\psi_2^\dagger(0) \psi_8'(0)]^\dagger \rangle, \end{aligned} \quad (\text{A2})$$

the correlation function is rewritten as,

$$\begin{aligned} \langle [-(\psi_1^\dagger \psi_7 + \psi_3^\dagger \psi_5) + (\psi_2^\dagger \psi_8 + \psi_4^\dagger \psi_6)] [-(\psi_1^\dagger \psi_7 + \psi_3^\dagger \psi_5) + (\psi_2^\dagger \psi_8 + \psi_4^\dagger \psi_6)]^\dagger \rangle \\ = \langle [(\psi_1^\dagger \psi_7' + \psi_3^\dagger \psi_5') + (\psi_2^\dagger \psi_8' + \psi_4^\dagger \psi_6')] [(\psi_1^\dagger \psi_7' + \psi_3^\dagger \psi_5') + (\psi_2^\dagger \psi_8' + \psi_4^\dagger \psi_6')]^\dagger \rangle. \end{aligned} \quad (\text{A3})$$

Therefore, $O_{\text{LSDW}_{\parallel,\text{out}}}$ in the response function can be expressed as

$$O_{\text{LSDW}_{\parallel,\text{out}}} = -\sum_{\sigma,\mu} \sigma \psi_{+,\sigma,\mu}^\dagger \psi_{-,\sigma,-\mu} \rightarrow \sum_{\sigma,\mu} \psi_{+,\sigma,\mu}^\dagger \psi'_{-,\sigma,-\mu}, \quad (\text{A4})$$

which leads to Eq. (2.17) with $\psi'_{p,\sigma,\mu}(x) = (1/\sqrt{2\pi\alpha}) \exp(ipk_{F\mu}x + i\Theta_{p,\sigma,\mu})$. The other order parameters are obtained in a similar way.

APPENDIX B: DERIVATION OF RENORMALIZATION GROUP EQUATIONS

We evaluate response functions by use of the renormalization group method.^{29,30} By treating the nonlinear terms in Eq. (2.9) as the perturbation, the response function for θ_{S+} field is calculated up to the third order as

$$\begin{aligned} \langle T_\tau \exp[(i/\sqrt{2})\theta_{S+}(x_1, \tau_1)] \exp[-(i/\sqrt{2})\theta_{S+}(x_2, \tau_2)] \rangle \\ = e^{-(K_S/2)U(r_1^F - r_2^F)} + \sum_{\nu=\rho,\sigma} \frac{1}{(4\pi)^2 \tilde{v}_\nu^2} \sum_{\epsilon=\pm 1} \int \frac{d^2 r_3^\nu}{\alpha^2} \frac{d^2 r_4^\nu}{\alpha^2} e^{-(K_S/2)U(r_1^F - r_2^F)} e^{-2K_\nu U(r_3^\nu - r_4^\nu)} \\ \times (G_{\nu+,S+}^2 e^{-2K_S U(r_3^F - r_4^F)} \{e^{\epsilon K_S [U(r_1^F - r_3^F) - U(r_1^F - r_4^F) - U(r_2^F - r_3^F) + U(r_2^F - r_4^F)]} - 1\} \\ + G_{\nu+,S-}^2 e^{-(2/K_S)U(r_3^F - r_4^F)} \{e^{i\epsilon [U(r_1^F - r_3^F) - U(r_1^F - r_4^F) - U(r_2^F - r_3^F) + U(r_2^F - r_4^F)]} - 1\}) \\ + \frac{1}{(4\pi)^2} \sum_{\epsilon=\pm 1} \int \frac{d^2 r_3^F}{\alpha^2} \frac{d^2 r_4^F}{\alpha^2} e^{-(K_S/2)U(r_1^F - r_2^F)} [(G_{C+,S+}^2 e^{-2K_C U(r_3^F - r_4^F)} \cos 2q_0(x_3 - x_4) + G_{C-,S+}^2 e^{-(2/K_C)U(r_3^F - r_4^F)}] \\ \times e^{-2K_S U(r_3^F - r_4^F)} \{e^{\epsilon K_S [U(r_1^F - r_3^F) - U(r_1^F - r_4^F) - U(r_2^F - r_3^F) + U(r_2^F - r_4^F)]} - 1\} \\ + [G_{C+,S-}^2 e^{-2K_C U(r_3^F - r_4^F)} \cos 2q_0(x_3 - x_4) + G_{C-,S-}^2 e^{-(2/K_C)U(r_3^F - r_4^F)}] \\ \times e^{-(2/K_S)U(r_3^F - r_4^F)} \{e^{i\epsilon [U(r_1^F - r_3^F) - U(r_1^F - r_4^F) - U(r_2^F - r_3^F) + U(r_2^F - r_4^F)]} - 1\}) \\ - \sum_{\nu=\rho,\sigma} \frac{4}{(4\pi)^3 \tilde{v}_\nu^3} \sum_{\epsilon=\pm 1} \int \frac{d^2 r_3^F}{\alpha^2} \frac{d^2 r_4^\nu}{\alpha^2} \frac{d^2 r_5^\nu}{\alpha^2} e^{-(K_S/2)U(r_1^F - r_2^F)} e^{-2K_\nu U(r_4^\nu - r_5^\nu)} \\ \times [(G_{\nu+,C+} + G_{\nu+,S+} + G_{C+,S+} e^{-2K_C U(r_3^F - r_5^F)} \cos 2q_0(x_3 - x_5) + G_{\nu+,C-} - G_{\nu+,S+} + G_{C-,S+} e^{-(2/K_C)U(r_3^F - r_5^F)}] e^{-2K_S U(r_3^F - r_4^F)} \\ \times \{e^{\epsilon K_S [U(r_1^F - r_3^F) - U(r_1^F - r_4^F) - U(r_2^F - r_3^F) + U(r_2^F - r_4^F)]} - 1\} + [G_{\nu+,C+} + G_{\nu+,S-} - G_{C+,S-} e^{-2K_C U(r_3^F - r_5^F)} \cos 2q_0(x_3 - x_5) \\ + G_{\nu+,C-} - G_{\nu+,S-} - G_{C-,S-} e^{-(2/K_C)U(r_3^F - r_5^F)}] e^{-(2/K_S)U(r_3^F - r_4^F)} \{e^{i\epsilon [U(r_1^F - r_3^F) - U(r_1^F - r_4^F) - U(r_2^F - r_3^F) + U(r_2^F - r_4^F)]} - 1\}) + \dots, \quad (\text{B1}) \end{aligned}$$

where $U(r_i^\nu - r_j^\nu) = \ln[\sqrt{(x_i - x_j)^2 + v_\nu^2(\tau_i - \tau_j)^2}/\alpha]$ for $i, j = 1, 2, 3, 4$, $d^2 r^\nu = v_\nu dx d\tau = v_\nu dx d\tau$ ($\nu = \rho, \sigma$ and F) and $q_0 \equiv 2t/v_F$. In order to obtain scaling equations of the coupling constants up to the second order, we need to calculate response

functions up to the third order for the nonlinear terms. Note that these terms do not exist in the one-dimensional case.²⁸ By putting $r_5=r_4+r$ and $r_5=r_3+r$, and expanding near $r=0$, we obtain the following renormalization in terms of effective quantities,

$$\begin{aligned} K_S^{\text{eff}} = & K_S - \frac{1}{2} \sum_{\nu=\rho,\sigma} G_{\nu+,S}^2 K_S^2 \int \frac{dr^F}{\alpha} \left(\frac{r^F}{\alpha} \right)^{3-2K_\nu-2K_S} + \frac{1}{2} \sum_{\nu=\rho,\sigma} G_{\nu+,S-}^2 \int \frac{dr^F}{\alpha} \left(\frac{r^F}{\alpha} \right)^{3-2K_\nu-2K_S} \\ & - \frac{1}{2} G_{C+,S}^2 K_S^2 \int \frac{dr^F}{\alpha} \left(\frac{r^F}{\alpha} \right)^{3-2K_C-2K_S} J_0(2q_0 r^F) + \frac{1}{2} G_{C+,S-}^2 \int \frac{dr^F}{\alpha} \left(\frac{r^F}{\alpha} \right)^{3-2K_C-2K_S} J_0(2q_0 r^F) \\ & - \frac{1}{2} G_{C-,S}^2 K_S^2 \int \frac{dr^F}{\alpha} \left(\frac{r^F}{\alpha} \right)^{3-2/K_C-2K_S} + \frac{1}{2} G_{C-,S-}^2 \int \frac{dr^F}{\alpha} \left(\frac{r^F}{\alpha} \right)^{3-2/K_C-2K_S}, \end{aligned} \quad (\text{B2})$$

$$G_{\nu+,S_p}^{\text{eff}}{}^2 = G_{\nu+,S_p}^2 - 2G_{C+,S_p} G_{\nu+,C+} G_{\nu+,S_p} \int \frac{dr^F}{\alpha} \left(\frac{r^F}{\alpha} \right)^{1-2K_C} J_0(2q_0 r^F) - 2G_{C-,S_p} G_{\nu+,C-} G_{\nu+,S_p} \int \frac{dr^F}{\alpha} \left(\frac{r^F}{\alpha} \right)^{1-2K_C}, \quad (\text{B3})$$

$$G_{C_p,S_{p'}}^{\text{eff}}{}^2 = G_{C_p,S_{p'}}^2 - \sum_{\nu=\rho,\sigma} \frac{2}{v_\nu} G_{C_p,S_{p'}} G_{\nu+,C_p} G_{\nu+,S_{p'}} \int \frac{dr^\nu}{\alpha} \left(\frac{r^\nu}{\alpha} \right)^{1-2K_\nu}, \quad (\text{B4})$$

where $r^\nu = [x^2 + (v_\nu \tau)^2]^{1/2}$, $\tilde{v}_\nu = v_\nu/v_F$ and $p, p' = \pm$. The second and third terms of the right-hand side in Eqs. (B3) and (B4) are obtained by exponentiating the third-order terms of Eq. (B1). For the transformation given by $\alpha \rightarrow \alpha' = \alpha e^{dl}$,²⁸ these quantities are scaled as

$$K_S^{\text{eff}}(K', G', q'_0, \alpha') = K_S^{\text{eff}}(K, G, q_0, \alpha), \quad (\text{B5})$$

$$G_{\nu p, \nu' p'}^{\text{eff}}(K', G', q'_0, \alpha') = G_{\nu p, \nu' p'}^{\text{eff}}(K, G, q_0, \alpha) (\alpha'/\alpha)^{\gamma_{\nu p, \nu' p'}}, \quad (\text{B6})$$

where K', G' , and q'_0 denote renormalized quantities. The exponent $\gamma_{\nu p, \nu' p'}$ is given by $\gamma_{\nu p, \nu' p'} = 2 - K_\nu^p - K_{\nu'}^{p'}$. By applying this infinitesimal transform to Eqs. (B2), (B3), and (B4), we obtain renormalization equations given by Eqs. (2.12), (2.14), and (2.15), respectively. In a similar way, the renormalization group equation for $K_\nu(l)$ ($\nu = \rho, \sigma$, and C) is calculated from the response function given by $\langle T_\tau e^{(i/\sqrt{2})\theta_{\nu\pm}(x_1, \tau_1)} e^{-(i/\sqrt{2})\theta_{\nu\pm}(x_2, \tau_2)} \rangle$ and the equations for $G_{\nu+,C\pm}(l)$ and $G_{\nu+,S\pm}(l)$ ($\nu = \rho$ and σ) are calculated from the response function for $\theta_{\nu\pm}$ field.¹⁹ We note that, in case of $t=0$, these equations become equal to the one-dimensional equations.¹⁸

The renormalization equation for $\tilde{t}(l)$ is derived by evaluating the difference of the density between two bands ($\mu = \pm$), which is given by

$$\begin{aligned} \Delta n \equiv & 2(k_{F+} - k_{F-})\alpha + 2\frac{T}{L} \int dx d\tau (\tilde{k}_{F+} - \tilde{k}_{F-})\alpha \\ = & -2q_0\alpha + \sqrt{2} \frac{T}{L} \alpha \int dx d\tau \langle \partial_x \theta_{C+}(x, \tau) \rangle \\ = & -2q_0\alpha + \sum_{\nu=\rho,\sigma} \frac{4}{\alpha} G_{\nu+,C+} K_C \frac{T}{L} \int dx d\tau \langle x \sin(\sqrt{2}\theta_{C+} - 2q_0x) \cos\sqrt{2}\theta_{\nu+} \rangle \\ & + \sum_{p=\pm} \frac{4}{\alpha} G_{C+,S_p} K_C \frac{T}{L} \int dx d\tau \langle x \sin(\sqrt{2}\theta_{C+} - 2q_0x) \cos\sqrt{2}\theta_{S_p} \rangle \\ = & -2q_0\alpha + \sum_{\nu=\rho,\sigma} G_{\nu+,C+}^2 K_C \int \frac{dr^F}{\alpha} \left(\frac{r^F}{\alpha} \right)^{2-2K_C-2K_\nu} J_1(2q_0 r^F) \\ & + \sum_{p=\pm} G_{C+,S_p}^2 K_C \int \frac{dr^F}{\alpha} \left(\frac{r^F}{\alpha} \right)^{2-2K_C-2K_S^p} J_1(2q_0 r^F) + \dots, \end{aligned} \quad (\text{B7})$$

where $4(\tilde{k}_{F+} - \tilde{k}_{F-})/2\pi \equiv \sum_{p,\sigma,\mu} \mu \psi_{p,\sigma,\mu}^\dagger \psi_{p,\sigma,\mu}$. The assumption of scaling invariance of Eq. (B7) with respect to infinitesimal transformation $\alpha' = \alpha e^{dl}$ leads to Eq. (2.16).

The response functions are calculated in terms of the solutions of Eqs. (2.10)–(2.16). The response function for $O_{SS_{\perp,\text{in}}}$, which is defined by $R_{SS_{\perp,\text{in}}}(x_1 - x_2, \tau_1 - \tau_2) \equiv \langle T_\tau O_{SS_{\perp,\text{in}}}(x_1, \tau_1) O_{SS_{\perp,\text{in}}}^\dagger(x_2, \tau_2) \rangle$, is calculated by writing $R_{SS_{\perp,\text{in}}}(x, \tau)$

$\equiv R_{SS_{\perp, \text{in}}}^{(0)}(x, \tau) F_{SS_{\perp, \text{in}}}(x, \tau)$, where $R_{SS_{\perp, \text{in}}}^{(0)}(x, \tau) = (\alpha/\sqrt{x^2 + v_{\rho}^2 \tau^2})^{1/2K_{\rho}} (\alpha/\sqrt{x^2 + v_{\sigma}^2 \tau^2})^{K_{\sigma}/2} (\alpha/\sqrt{x^2 + v_F^2 \tau^2})^{(1/K_C + K_S)/2}$. By assuming the scaling relation $F_{SS_{\perp, \text{in}}}[r, \alpha(l), K_{\nu}(l), G(l)] = I_{SS_{\perp, \text{in}}}[dl, K_{\nu}(l), G(l)]$, $F_{SS_{\perp, \text{in}}}[r, \alpha(l+dl), K_{\nu}(l+dl), G(l+dl)]$, the multiplicative factor $I_{SS_{\perp, \text{in}}}$ is written as,

$$\begin{aligned} I_{SS_{\perp, \text{in}}} = & \exp \left(-G_{\sigma+, C-} dl + G_{\sigma+, S+} dl + G_{C-, S+} dl + \frac{1}{4\tilde{v}_{\rho}^2} \{ -G_{\rho+, C+}^2 J_0(2q_0\alpha) - G_{\rho+, C-}^2 - G_{\rho+, S+}^2 - G_{\rho+, S-}^2 \} U(r_1^{\rho} - r_2^{\rho}) dl \right. \\ & + \frac{1}{4\tilde{v}_{\sigma}^2} K_{\sigma}^2 [G_{\sigma+, C+}^2 J_0(2q_0\alpha) + G_{\sigma+, C-}^2 + G_{\sigma+, S+}^2 + G_{\sigma+, S-}^2] U(r_1^{\sigma} - r_2^{\sigma}) dl \\ & + \frac{1}{4} \left\{ \sum_{\nu=\rho, \sigma} [-G_{\nu+, C+}^2 J_0(2q_0\alpha) + G_{\nu+, C-}^2 / K_C^2 + G_{\nu+, S+}^2 K_S^2 - G_{\nu+, S-}^2] + G_{C+, S+}^2 (-1 + K_S^2) J_0(2q_0\alpha) \right. \\ & \left. + G_{C+, S-}^2 (-2) J_0(2q_0\alpha) + G_{C-, S+}^2 (1/K_C^2 + K_S^2) + G_{C-, S-}^2 (1/K_C^2 - 1) \right\} U(r_1^F - r_2^F) dl \Big), \end{aligned} \quad (\text{B8})$$

which leads to $F_{SS_{\perp, \text{in}}}$ expressed as

$$F_{SS_{\perp, \text{in}}}(r, K, G) = \exp \left(\sum_{l=0}^{\ln(r/\alpha)} \ln \{ I_{SS_{\perp, \text{in}}}[dl, K(l), G(l)] \} \right). \quad (\text{B9})$$

We note that terms including the second order of the coupling constants are rewritten in a simple form. For example, one obtains

$$\begin{aligned} & \frac{1}{4} \int dl \left\{ \sum_{\nu=\rho, \sigma} [-G_{\nu+, C+}^2 J_0(2q_0\alpha) + G_{\nu+, C-}^2 / K_C^2 + G_{\nu+, S+}^2 K_S^2 - G_{\nu+, S-}^2] + G_{C+, S+}^2 (-1 + K_S^2) J_0(2q_0\alpha) \right. \\ & \quad \left. + G_{C+, S-}^2 (-2) J_0(2q_0\alpha) + G_{C-, S+}^2 (1/K_C^2 + K_S^2) + G_{C-, S-}^2 (1/K_C^2 - 1) \right\} \ln \left[\frac{r}{\alpha(l)} \right] \\ & = \frac{1}{2} \int dl \left\{ \frac{1}{K_C^2(l)} \frac{dK_C(l)}{dl} - \frac{dK_S(l)}{dl} \right\} \ln \left[\frac{r}{\alpha(l)} \right] \\ & = \frac{1}{2} \left\{ \frac{1}{K_C(0)} + K_S(0) \right\} \ln \left(\frac{r}{\alpha} \right) - \int_0^{\ln(r/\alpha)} dl \left\{ \frac{1}{K_C(l)} + K_S(l) \right\}, \end{aligned} \quad (\text{B10})$$

where $\alpha(l) = \alpha e^l$. Thus, the normalized response function $\bar{R}_{SS_{\perp, \text{in}}}(x, \tau) [\equiv R_{SS_{\perp, \text{in}}}(x, \tau) \cdot 2(\pi\alpha)^2]$, is expressed as,

$$\begin{aligned} \bar{R}_{SS_{\perp, \text{in}}}(x, \tau) = & \exp \left[\int_0^{\ln \sqrt{x^2 + (v_{\rho}\tau)^2} / \alpha} dl \left(-\frac{1}{2} \frac{1}{K_{\rho}(l)} \right) \right] \\ & \times \exp \left\{ \int_0^{\ln \sqrt{x^2 + (v_{\sigma}\tau)^2} / \alpha} dl \left[-\frac{1}{2} K_{\sigma}(l) - \frac{1}{\tilde{v}_{\sigma}} G_{\sigma+, C-}(l) + \frac{1}{\tilde{v}_{\sigma}} G_{\sigma+, S+}(l) \right] \right\} \\ & \times \exp \left(\int_0^{\ln \sqrt{x^2 + (v_F\tau)^2} / \alpha} dl \left\{ -\frac{1}{2} \left[\frac{1}{K_C(l)} + K_S(l) \right] + G_{C-, S+}(l) \right\} \right), \end{aligned} \quad (\text{B11})$$

which leads to Eq. (2.22). Other response functions are obtained in a similar way. In deriving Eqs. (2.20)–(2.22), we replaced v_{ρ} and v_{σ} by v_F , which may cause a slight deviation of the numerical factor.

¹D. Jérôme and H. J. Schulz, Adv. Phys. **31**, 299 (1982).

²K. Bechgaard and D. Jérôme, Phys. Scr. **T39**, 37 (1991).

³G. Grüner, Rev. Mod. Phys. **66**, 1 (1994).

⁴C. Bourbonnais, J. Phys. I **3**, 413 (1993); P. Wzietek, F. Creuzet, C. Bourbonnais, D. Jérôme, K. Bechgaard, and P. Batail, *ibid.* **3**, 171 (1993).

⁵J. Moser, M. Gabay, P. Auban-Senzier, D. Jérôme, K. Bechgaard, and J. M. Fabre, Eur. Phys. J. B **1**, 39 (1998).

⁶V. J. Emery, R. Bruinsma, and S. Barišić, Phys. Rev. Lett. **48**, 1039 (1982).

⁷A. Schwartz, S. Donovan, M. Dressel, L. Degiorgi, and G. Grüner, Synth. Met. **86**, 2129 (1997).

- ⁸V. Vescoli, L. Degiorgi, W. Henderson, G. Grüner, K. P. Sarkey, and L. K. Montgomery, *Science* **281**, 1181 (1998).
- ⁹V. M. Yakovenko, *Pis'ma Zh. Éksp. Teor. Fiz.* **56**, 523 (1992) [*JETP Lett.* **56**, 510 (1992)].
- ¹⁰C. Bourbonnais, *Mol. Cryst. Liq. Cryst.* **119**, 11 (1985); C. Bourbonnais and L. G. Caron, *Int. J. Mod. Phys. B* **5**, 1033 (1991).
- ¹¹A. A. Nersesyan, A. Luther, and F. V. Kusmartsev, *Phys. Lett. A* **176**, 363 (1993).
- ¹²M. Fabrizio, *Phys. Rev. B* **48**, 15 838 (1993).
- ¹³A. M. Finkel'stein and A. I. Larkin, *Phys. Rev. B* **47**, 10 461 (1993).
- ¹⁴H. Yoshioka and Y. Suzumura, *J. Low Temp. Phys.* **106**, 49 (1997).
- ¹⁵D. V. Khveshchenko and T. M. Rice, *Phys. Rev. B* **50**, 252 (1994).
- ¹⁶H. J. Schulz, *Phys. Rev. B* **53**, R2959 (1996).
- ¹⁷L. Balents and M. P. A. Fisher, *Phys. Rev. B* **53**, 12 133 (1996).
- ¹⁸J. Sólyom, *Adv. Phys.* **28**, 201 (1979).
- ¹⁹M. Tsuchiizu and Y. Suzumura, *Physica C* **303**, 246 (1998).
- ²⁰P. W. Anderson *Phys. Rev. Lett.* **67**, 3844 (1991).
- ²¹D. G. Clarke, S. P. Strong, and P. W. Anderson, *Phys. Rev. Lett.* **72**, 3218 (1994).
- ²²S. P. Strong, D. G. Clarke, and P. W. Anderson, *Phys. Rev. Lett.* **73**, 1007 (1994).
- ²³C. Bourbonnais, in *Strongly Interacting Fermions and High T_c Superconductivity*, edited by B. Doucot and J. Zinn-Justin (Elsevier, Amsterdam, 1995), p. 307.
- ²⁴T. Giamarchi, *Physica B* **230-232**, 975 (1997), and references therein.
- ²⁵A. Schwartz, M. Dressel, G. Grüner, V. Vescoli, L. Degiorgi, and T. Giamarchi, *Phys. Rev. B* **58**, 1261 (1998).
- ²⁶Y. Suzumura, M. Tsuchiizu, and G. Grüner, *Phys. Rev. B* **57**, R15 040 (1998).
- ²⁷J. Kishine and K. Yonemitsu, *J. Phys. Soc. Jpn.* **67**, 2590 (1998).
- ²⁸T. Giamarchi and H.J. Schulz, *J. Phys. (France)* **49**, 819 (1988).
- ²⁹T. Giamarchi and H. J. Schulz, *Phys. Rev. B* **39**, 4620 (1989).
- ³⁰M. Tsuchiizu, H. Yoshioka, and Y. Suzumura, *Prog. Theor. Phys.* **98**, 1045 (1997).
- ³¹The second term of the right-hand side of Eq. (2.16) is corrected to be twice as large as that of the previous paper (Ref. 26). The resultant region of confinement becomes slightly large.
- ³²T. B. Bahder and F. Woynarovich, *Phys. Rev. B* **33**, 2114 (1986).
- ³³M. Mori and H. Fukuyama, *J. Phys. Soc. Jpn.* **65**, 3604 (1996).
- ³⁴Y. Suzumura, M. Tsuchiizu, and G. Grüner (unpublished).